DOI: 10.6060/mhc224792d

Boron Subphthalocyanines Bearing Non-Steroidal Anti-Inflammatory Drug Diclofenac: Synthesis and Photochemical Properties

Tatiana V. Dubinina,[a@] Ivan D. Burtsev,[b] Alina S. Agranat,[a] Anton E. Egorov,[b] Alexey A. Kostyukov,[b] Vladimir A. Kuzmin,[b] and Elena R. Milaeva[a]

[a]*Department of Chemistry, Lomonosov Moscow State University, 119991 Moscow, Russian Federation*
[b]*Emanuel Institute of Biochemical Physics, Russian Academy of Sciences, 119334 Moscow, Russian Federation*
[@]*E-mail: dubinina.t.vid@gmail.com*

Dedicated to Professor I. P. Beletskaya on the occasion of her Anniversary

Phenyl and phenoxy-substituted boron subphthalocyanines were decorated by non-steroidal anti-inflammatory drug diclofenac using axial exchange reaction. Target complexes show high values of singlet oxygen generation (Φ_Δ = 0.44–0.55) and fluorescence quantum yields (Φ_F = 0.20–0.33). The flash photolysis method allowed us to detect and characterize the triplet states of subphthalocyanines. In the case of phenoxy-substituted subphthaloyanine, introduction of diclofenac results in pronounced increase in fluorescence quantum yield.

Keywords: Boron, subphthalocyanines, non-steroidal anti-inflammatory drugs, diclofenac, photochemistry.

Субфталоцианины бора, содержащие нестероидный противовоспалительный препарат диклофенак: синтез и фотохимические свойства

Т. В. Дубинина,[a@] И. Д. Бурцев,[b] А. С. Агранат,[a] А. Е. Егоров,[b] А. А. Костюков,[b] В. А. Кузьмин,[b] Е. Р. Милаева[a]

[a]*Химический факультет, Московский государственный университет имени М.В. Ломоносова, 119991 Москва, Российская Федерация*
[b]*Институт биохимической физики им. Н.М. Эмануэля РАН, 119334 Москва, Российская Федерация*
[@]*E-mail: dubinina.t.vid@gmail.com*

С использованием реакции обмена аксиального лиганда в молекулы фенил- и феноксизамещенных субфталоцианинов бора введен нестероидный противовоспалительный препарат диклофенак. Целевые соединения демонстрируют высокие значения выходов генерации синглетного кислорода (Φ_Δ = 0,44–0,55) и квантового выхода флуоресценции (Φ_F = 0,20–0,33). Метод флэш-фотолиза позволил обнаружить и охарактеризовать триплетные состояния субфталоцианинов. В случае феноксизамещенного субфталоцианина введение препарата диклофенак приводит к выраженному увеличению квантового выхода флуоресценции.

Ключевые слова: Бор, субфталоцианины, нестероидные противовоспалительные препараты, диклофенак, фотохимия.

Introduction

Boron subphthalocyanines exhibit low aggregation propensity, bright fluorescence, and high yields of singlet oxygen generation.[1,2] These brilliant properties result from nonplanar cone-shaped structure of these molecules.[3,4] Until recently, subphthalocyanines have been studied as promising materials for dye sensitized solar cells,[5-8] highly

sensitive sensors[9-11] and materials for nonlinear optics.[12,13] However, they demonstrate high potential for application in photodynamic therapy and fluorescent visualization.[14-17] Introduction of different peripheral functional groups into subphthalocyanine macrocycle or axial ligand exchange allows to tune optical and photochemical properties of boron subphthalocyanines.[18,19] Functionalization of the subphthalocyanine molecule can be achieved in the starting dinitriles up to the stage of template cyclization or in the formed macrocycle using a *post*synthetic strategy.[20] The introduction of bulky axial ligands increases the solubility and bioavailability of sub-phthalocyanines.[21,22] In addition, the mild reaction conditions of the axial ligand exchange expand the range of functional groups that can be used for this procedure.[19,21] In the recent paper of J. Demuth *et al.* the increase of phototoxicity was demonstrated for axially substituted boron subphthalocyanines.[16] An interesting way of axial functionalization of subphthalocyanine molecules is decorating with physiologically active compounds. However, only a few examples of subphthalocyanines of this type are described in the literature.[16,23] The present paper focuses on the synthesis and photochemical properties of subphthalo-cyanines bearing diclofenac as an axial ligand. The presence of a non-steroidal anti-inflammatory drug in the subphthalocyanine molecule can initiate the appearance of dual pharmacological properties in target molecules. These studies are a preliminary step before *in vitro* studies and have the main goal of showing the possibility of generating singlet oxygen by subphthalocyanines containing diclofenac. As objects of structural modification, we chose two symmetrically substituted boron subphthalocyanines (phenyl- and phenoxy substituted). These subphthalo-cyanines have shown good yields of singlet oxygen generation[12,24] in previous studies and may be good lead compounds for further functionalization.

Experimental

Hexaphenylsubphthalocyanine boron chloride, and hexaphenoxysubphthalocyanine boron chloride were obtained using template synthesis by analogy with the previously published method.[12,25] Diclofenac acid was prepared from corresponding sodium salt using the standard protocol of hydrolysis.[26,27] N,N-Diisopropylethylamine (Sigma-Aldrich, *ReagentPlus*®, ≥99%), silver trifluoromethanesulfonate (Sigma-Aldrich, ≥99%), phenol (Sigma-Aldrich, ≥99%) were used without additional purification. All reactions were monitored by TLC and/or UV-Vis spectroscopy until the complete disappearance of the starting subphthalocyanines unless otherwise specified. TLC was performed using TLC aluminum sheets (silica gel layer, ALUGRAM SIL G UV_{254}, 20×20 cm, MACHEREY-NAGEL). Matrix assisted laser desorption/ionization time-of-flight (MALDI-TOF) mass spectra were measured on a Bruker Autoflex II mass spectrometer without matrix. ^{1}H and ^{11}B NMR spectra were recorded on a Bruker AVANCE 600 spectrometer. Chemical shifts are given in ppm relative to $SiMe_4$. In the case of ^{11}B NMR, $BF_3 \times Et_2O$ was used as external standard.

UV-visible and fluorescence spectroscopy

UV-vis absorption spectra were recorded on a Shimadzu UV-3101PC spectrophotometer (Japan) in the range of 300–800 nm in a quartz cuvette with an optical pathlength of 1 cm at room temperature.

The fluorescence spectra were recorded using a FluoTime 300 fluorescence lifetime spectrometer (PicoQuant GmbH, Germany) with a xenon lamp as an excitation source in a 1.0×1.0 cm quartz cuvette at room temperature.

Fluorescence lifetime measurements

The fluorescence decay curves of SubPcs were obtained with a FluoTime 300 fluorescence lifetime spectrometer (PicoQuant GmbH, Germany) by a picosecond time-correlated single photon counting (TCSPC) and a SOLEA laser. The instrument response function (IRF) was obtained using Ludox (DuPont) as a scattering standard. All experiments were carried out at room temperature. The fluorescence decay was fitted by using the FluoFit software (PicoQuant GmbH, Germany). The fluorescence lifetimes were estimated by using a multi-exponential model according to the equation described in:[28]

$$I(t) = \int_{-\infty}^{t} IRF(t') \sum_{i=1}^{n} I_i e^{\left(\frac{-t-t'}{\tau_i}\right)} dt' \quad \text{(I)},$$

where I_i is the amplitude and τ_i is the lifetime of the *i*-th decay component, and *n* is the number of decay component. The goodness of fit was evaluated by χ^2 test (close to 1 for the best fit) as well as by the control of residuals and autocorrelation function.

Flash photolysis

The triplet-triplet absorption spectra and kinetics decay of subphthalocyanines were measured using a conventional flash photolysis setup: optical path length 20 cm quartz cuvettes, excitation was performed by a Xe-lamp (20 μs) through different blue and orange optical glass filters. Signals were recorded on a PMT-38 photomultiplier (MELZ, USSR) at 400–800 nm. All solutions were degassed before the experiments.

Singlet oxygen quantum yields

Singlet oxygen luminescence spectra were recorded in toluene using tetraphenylporphyrin (TPP; Φ_Δ = 0.66)[29] as a standard. The concentrations of the compounds were selected in the range of $(2.3 – 3.7) \cdot 10^{-6}$ M, while the optical density at the excitation wavelength was the same for all solutions.

The luminescence spectra of singlet oxygen in toluene (λ_{max} ~1270 nm) were obtained by irradiation with a Xe-lamp (photoexcitation at λ = 513 nm of solutions saturated with oxygen at room temperature).

The quantum yields of singlet oxygen were determined in toluene according to the formula:[30]

$$\Phi_\Delta^i = \frac{F^i A_s}{F^s A_i} \Phi_\Delta^s \quad \text{(II)},$$

where Φ_Δ^s is the quantum yield of singlet oxygen for the standard, *Fi* and F_S are the areas under the luminescence spectra of singlet oxygen for the sample and the standard, A_i and A_S are the optical absorption densities of the sample and the standard at the registration wavelength, respectively.

Fluorescence quantum yields

Fluorescence spectra were recorded using quartz cuvettes with an optical path length of 1 cm at room temperature. Quantum fluorescence yields of subphthalocyanines were recorded in *n*-propanol using rhodamine 6G as a standard (Φ_f = 0.96 in *n*-propanol[31]) irradiated with the xenon lamp at 505 nm.

To avoid the internal filter effect, the optical density of the standard and sample solutions at the excitation wavelength was not more than 0.1.

The quantum yields of fluorescence were determined by the method described in [32] according to the formula:

$$\Phi_f^i = \frac{F^i f_s n_i^2}{F^s f_i n_s^2} \Phi_f^s, \quad \text{(III)}$$

where Φ_f^S is the fluorescence quantum yield for the standard, F_i and F_S are the areas under the luminescence spectra of the sample and the standard, n_i^2 and n_s^2 are the squares of the refractive indices in the used solvent for the sample and standard, respectively. $f_i = 1 - 10^{-Ax}$, where A_x is the absorption of the sample at the excitation wavelength.

Synthesis

Preparation of boron subphthalocyanine ***2a*** *(PhSubPcB-DCF).* A mixture of hexaphenylsubphthalocyanine boron chloride **1a** (60.0 mg, 0.068 mmol) and silver trifluoromethanesulfonate (23.0 mg, 0.085 mmol) was stirred in dry toluene (1.5 mL) at room temperature under argon for 2.5 h. After the complete conversion of initial complex **1a** to corresponding triflate (TLC control, SiO_2, C_6H_6), diclofenac acid (40 mg, 0.135 mmol) and N,N-diisopropylethylamine (0.015 mL, 0.085 mmol) were added into the reaction mixture. The mixture was stirred at room temperature during 20h. Then the hexane was added to the reaction mixture and the precipitate was filtered off. Then the target compound was washed with benzene. The benzene solution was evaporated under reduced pressure. Additional purification was carried out using gel permeating chromatography (bio-beads SX-1, C_6H_6). The complex **2a** was obtained as a purple powder (65 mg, 83%). UV-Vis (CH_3CN) λ_{max} nm (lgε): 579 (4.36). ^{1}H NMR (600.13 MHz, $CDCl_3$) δ_H ppm: 3.76 (s, 2H, CH_2); 6.47–7.26 (m, 37H, SubPc and diclofenac aromatics); 7.46-7.88 (m, 6H, H_{Pc}); 8.59 (br.s, 1H, NH). ^{11}B NMR (192.55 MHz, $CDCl_3$) δ_B ppm: –14.84. MS-MALDI-TOF (negative mode) *m/z*: 1101 ([M-CO_2]$^-$, 85%); 1145 ([M]$^-$, 100%).

Preparation of boron subphthalocyanine ***2b*** *(PhOSubPcB-DCF).* A mixture of hexaphenoxysubphthalocyanine boron chloride **1b** (60.0 mg, 0.060 mmol) and silver trifluoromethanesulfonate (19.0 mg, 0.075 mmol) was stirred in dry toluene (1 mL) at room temperature under argon for 1.5 h. After the complete conversion of initial complex **1b** to corresponding triflate (TLC control, SiO_2, C_6H_6), diclofenac acid (35 mg, 0.12 mmol) and N,N-diisopropylethylamine (0.013 mL, 0.075 mmol) were added into the reaction mixture. The mixture was stirred at room temperature during 19h. Then the hexane was added to the reaction mixture and the precipitate was filtered off. Then the target compound was washed with benzene. The benzene solution was evaporated under reduced pressure. Additional purification was carried out using gel permeating chromatography (bio-beads SX-1, C_6H_6). The complex **2b** was obtained as a purple powder (60 mg, 81%). UV-Vis (CH_3CN) λ_{max} nm (lgε): 567 (4.00). ^{1}H NMR (600.13 MHz, $CDCl_3$) δ_H ppm: 3.73 (s, 2H, CH_2); 6.48–7.47 (m, 43H, SubPc and diclofenac aromatics); 7.78 (br.s, 1H, NH). ^{11}B NMR (192.55 MHz, $CDCl_3$) δ_B ppm: –15.31. MS-MALDI-TOF (negative mode) *m/z*: 1206 ([M-Cl]$^-$, 50%); 1241 ([M]$^-$, 90%); 1276 ([M+Cl]$^-$, 100%).

Results and Discussion

Synthesis

The protocol for introducing a diclofenac into the axial position of boron subphthalocyanines includes an intermediate stage of exchanging a chlorine atom for a good leaving group, triflate. Then the triflate group was removed with diclofenac in the presence of N,N-diisopropylethyl-amine (DIPEA) as a base. We chose silver trifluoro-methanesulfonate as the triflate source instead of trimethyl-silyl trifluoromethanesulfonate [21] because of the possibility of carrying out the reaction under mild conditions: fast process, room temperature. Target compounds **2a,b** were purified using gel permeation chromatography. This method was earlier successfully applied for introduction of isoleucine and substituted benzoic acids into the axial position of unsubstituted boron subphthalocyanine.[21]

The purity of the hybrid molecules has been proven by high resolution mass spectrometry and NMR spectroscopy.

MALDI-TOF mass spectra were measured for both positive and negative ion modes. However, we found that minimal fragmentation and better resolution was observed in the case of negative ion mode. Complexes **2** demonstrated intense molecular ions (Figure 1 and Supporting Information). Under the laser ionization cleavage of C-Cl bond in diclofenac moiety and fragmentation of CO_2 was observed. In addition, the formation of adduct with chlorine atom was also found for complex **2a**.

^{1}H NMR spectra for complexes **2** showed the overlapping of aromatic proton signals of subphthalocyanine periphery and diclofenac moiety (Figure 2 and Supporting Information). This statement is supported by the data of ^{1}H-^{1}H COSY NMR.

In ^{11}B NMR spectra of complexes **2** typical signals of boron atoms coordinated by nitrogen atoms were observed in the range -14 - -15 ppm.

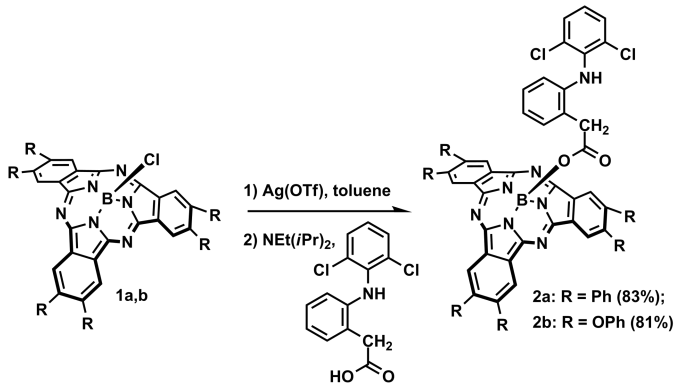

Scheme 1. Synthesis of subphthalocyanines **2a,b**.

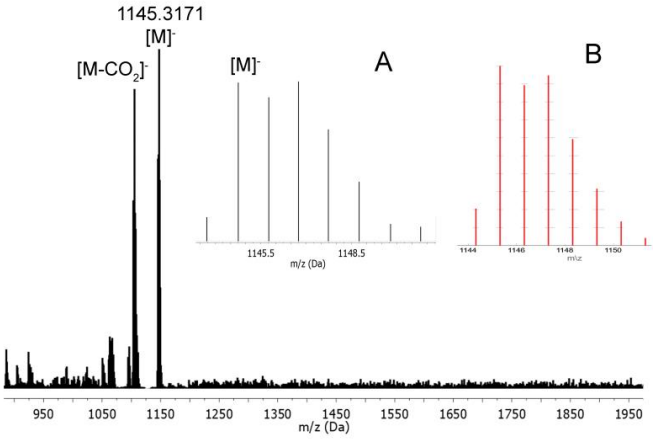

Figure 1. MALDI TOF mass spectrum (positive ion mode) of boron subphthalocyanine **2a**, isotopic pattern (inset A) and simulated MS pattern (inset B).

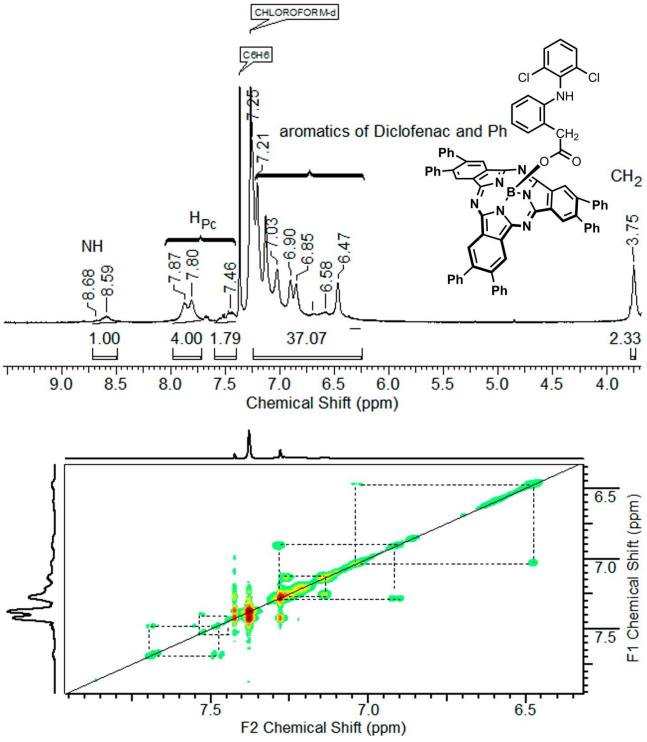

Figure 2. ^{1}H (A) and aromatic region of ^{1}H-^{1}H COSY (B) NMR spectra of boron subphthalocyanine **2a** measured in $CDCl_3$.

Table 1. UV-Vis, fluorescence and photochemical data for target compounds and literature data.

Compound	λ_{abs}, nm[a]	λ_{em}, nm[a]	Φ_f[a]	τ_f, ns[a]	τ_T, ms[b]	Φ_Δ[c]
^{Ph}SubPc-DCF **2a**	578	594	0.20	1.95	1.11	0.50
^{PhO}SubPc-DCF **2b**	567	580	0.33	1.94	1.24	0.44
^{Ph}SubPcCl **1a** [25]	582	600	0.27	2.88	3.10	0.58
^{PhO}SubPcCl **1b**[25]	572	582	0.13	2.90	1.43	0.48

[a] – spectra were measured in *n*-propanol; [b] – spectra were measured in CH_3CN; [c] – spectra were measured in toluene

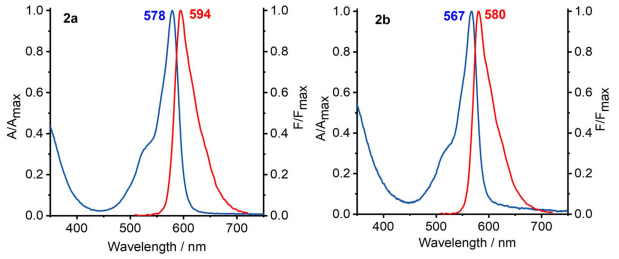

Figure 3. Normalized UV-Vis spectra (blue lines) and emission spectra (red lines) of subphthalocyanines **2** in *n*-propanol.

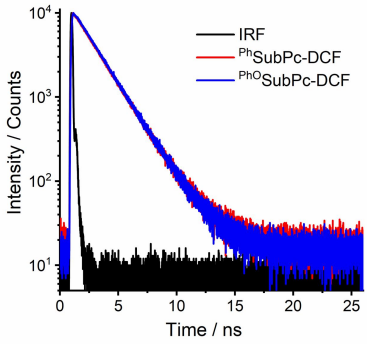

Figure 4. The fluorescence decay kinetics of boron subphthalocyanines in *n*-propanol. λ_{ex} = 520 nm, λ_{reg} = 580 nm.

UV-Vis spectroscopy and photochemistry

UV-Vis and fluorescence spectra of target hybrid molecules demonstrate intense absorption and fluorescence in visible region. The Stokes shifts lie in the range of 14 - 15 nm. The bathochromic shifts of absorption and fluorescence bands were observed going from phenoxy to phenyl-substituted complexes. It results from the increase of quantity of electron-releasing groups on the periphery of subphthalocyanine macrocycle.

Introduction of axial ligand only slightly influence on the position of *Q* band. About 3 nm bathochromic shift of *Q* band was observed going from complexes **2** to **1**. Similar regularity was found for fluorescence spectra. Fluorescence lifetimes are slightly lower for diclofenac-substituted complexes compared to compounds **1**. Whereas fluorescence quantum yields for complexes **2a** and **1a** are similar, Φ_f value for complex **2b** is about 3 times higher than for initial compound **1b** without diclofenac.

The kinetics of fluorescence decay (Figure 4) were studied. The values of the fluorescence lifetimes for the compounds **2** are on the order of 2 ns. It is slightly lower than corresponding ones for initial complexes **1**.

The data show that fluorescence decay kinetics of the complexes are mono-exponential, with $\chi^2 < 1.2$, which corresponds to the first-order reaction kinetics.

To study the ability of subphthalocyanines to generate reactive oxygen species under photoactivation the flash photolysis measurements were carried out. The spectral-kinetic parameters of the triplet states of boron subphthalocyanines in acetonitrile were determined.

Differential triplet-triplet absorption spectra demonstrate the bleaching of the *Q* band in the range 500 – 600 nm and the appearance of triplet bands in the ranges of 420 – 500 nm and 600 – 800 nm (Figure 5). The lifetimes of triplet state correspond primarily to the value of 1 ms (triplet decay rates k_T are listed in Table 2). The kinetics of the triplet state decay for the subphthalocyanine complexes are following mono-exponential dependence (k_T, reaction 4, Scheme 2).

Triplet molar extinction coefficients (ε_T) were calculated using singlet depletion method:

$$\varepsilon_T = \varepsilon\,(\Delta A_T / \Delta A_S), \qquad \text{(IV)}$$

where ΔA_T and ΔA_S are differential optical densities after the flash impulse at triplet absorption maximum and singlet bleaching minimum, respectively; ε is molar extinction coefficient of the ground state.

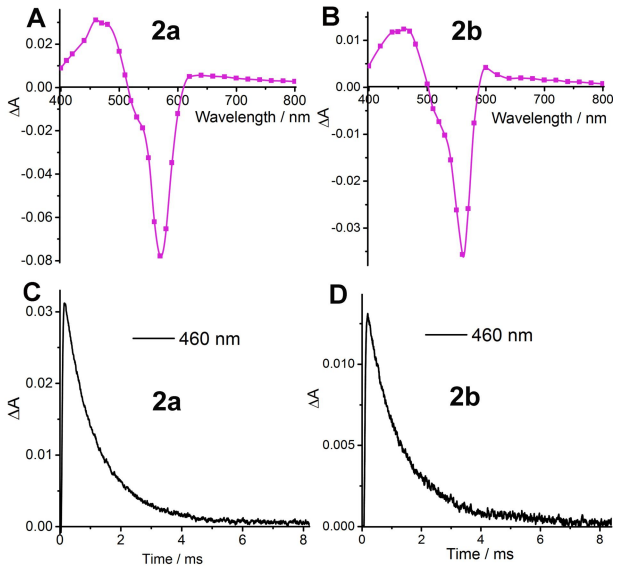

Figure 5. Differential triplet-triplet absorption spectra of solutions of subphthalocyanines **2a,b** in CH_3CN ($C = 1 \cdot 10^{-6}$ M, time after the flash 150 μs) (A,B). The kinetics of the triplet states decay at 460 nm (C, D).

$S_o + h\nu \rightarrow S_1$ (1)

$S_1 \rightarrow S_0 + h\nu_{fl}$ (2)

$S_1 \rightarrow T$ (3)

$T \rightarrow S_o$ (4) k_T

$T + {}^3O_2 \rightarrow S_o + {}^1O_2$ (5) k_q

Scheme 2.

Table 2. Spectral kinetic parameters of triplet states of target subphthalocyanines.

Compound	$\lambda_{max\ t\text{-}t}$, nm	$\lg\varepsilon_{Tmax}$, $M^{-1} \times cm^{-1}$	k_T, $s^{-1} \times 10^{-2}$
^{Ph}SubPc-DCF **2a**	460	3.96	9.0
^{PhO}SubPc-DCF **2b**	460	3.54	8.0

The quenching constant (k_q) of the triplet state by oxygen was calculated according to the equation:

$$k = k_T + k_q[O_2], \quad (V)$$

where k is the decay rate of the triplet state, k_T is the decay rate of the triplet state in the deoxygenated solution, k_q is the bimolecular oxygen quenching constant. Oxygen quenching constant in acetonitrile is estimated to be $k_q = 1.9 \cdot 10^9$ $M^{-1} \cdot s^{-1}$ for all compounds, which is close to the value of the diffusion rate constant in this solvent, accounting the spin-statistical factor 1/9.

The results of flash photolysis measurements were supported by the measurements of $^1O_2$ quantum yields. Scheme 2 illustrates the mechanism of photochemical processes involving subphthalocyanines, including singlet oxygen formation under irradiation. Singlet oxygen is generated as a result of energy transfer from the photosensitizer triplet state (T) to oxygen molecules in the ground state (equation 5, Scheme 2).

Singlet oxygen quantum yields (Φ_Δ) were determined using the relative method of $^1O_2$ phosphorescence at 1270 nm (Table 1, Figure 6). The tetraphenylporphyrin (TPP) was chosen as a reference compound.

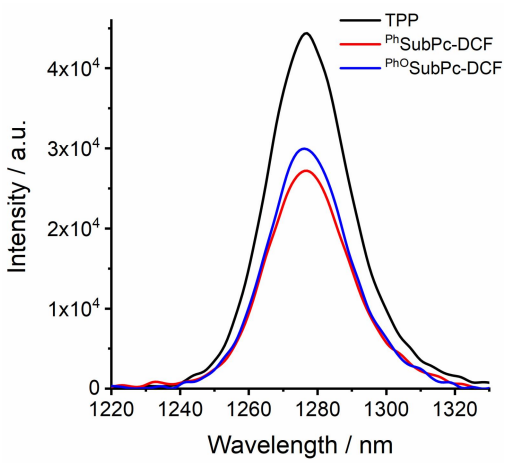

Figure 6. Luminescence spectra of singlet oxygen in the solutions of subphthalocyanines **2** and reference compound (TPP) (λ_{ex}=513 nm).

Resulting Φ_Δ values for complexes **2** are similar to initial compounds **1**. In contrast to fluorescence quantum yields the singlet oxygen quantum yields increase from ^{PhO}SubPc-DCF to ^{Ph}SubPc-DCF. This regularity can be explained by the competition between the fluorescence and singlet oxygen generation processes. Also, the presence of phenoxy and phenyl substituents leads to an increase in the contribution of vibrational relaxation, which is expressed in a decrease in the contribution of the internal conversion process. The contribution of intersystem crossing decreases, which leads to a decrease in the quantum yield of singlet oxygen for compounds with such substituents.

Conclusions

New hybrid photosensitizers consisting of a subphthalocyanine unit and a diclofenac molecule in the axial position are presented. Two types (aryl, and aryloxy) of peripheral substituents were chosen to study the correlation between the structure of photosensitizers and their optical properties. It has been found that the ability to generate singlet oxygen and the fluorescent properties of subphthalocyanines change in the opposite way. Singlet oxygen quantum yields are similar for initial boron subphthalocyanines and diclofenac-substituted complexes (Φ_Δ~0.4 – 0.5). However, the introduction of diclofenac fragment into phenoxy-substituted subphthalocyanine led to an increase in the fluorescence yield (Φ_f= 0.33).

Acknowledgements. Synthesis of target boron subphthalocyanines was supported by Russian Science Foundation Project no. 22-63-00016. Spectral measurements were carried out in the Core Facility of the Institute of Biochemical Physics RAS “New Materials and Technologies”. The study was supported by the RF State Program for IBCP RAS, Project no. 1201253303.

References

1. Claessens C.G., González-Rodríguez D., Rodríguez-Morgade M.S., Medina A., Torres T. *Chem. Rev.* **2014**, *114*, 2192–2277.

2. Lavarda G., Labella J., Martínez-Díaz M.V., Rodríguez-Morgade M.S., Osuka A., Torres T. *Chem. Soc. Rev.* **2022**, *51*, 9482–9619.
3. Fulford M.V., Jaidka D., Paton A.S., Morse G.E., Brisson E.R.L., Lough A.J., Bender T.P. *J. Chem. Eng. Data* **2012**, *57*, 2756–2765.
4. Potz R., Göldner M., Hückstädt H., Cornelissen U., Tutaß A., Homborg H. *Z. Anorg. Allg. Chem.* **2000**, *626*, 588–596.
5. Cnops K., Rand B.P., Cheyns D., Verreet B., Empl M.A., Heremans P. *Nat. Commun.* **2014**, *5*, 3406.
6. Maklakov S.S., Dubinina T.V., Osipova M.M., Petrusevich E.F., Mishin A.D., Tomilova L.G. *J. Porphyrins Phthalocyanines* **2016**, *20*, 1134–1141.
7. Sulas D.B., Rabe E.J., Schlenker C.W. *J. Phys. Chem. C* **2017**, *121*, 26667–26676.
8. Stuzhin P.A., Mikhailov M.S., Travkin V.V., Gudkov E.Y., Pakhomov G.L. *Macroheterocycles* **2012**, *5*, 162–165.
9. Skvortsov I.A., Zimcik P., Stuzhin P.A., Novakova V. *Dalton Trans.* **2020**, *49*, 11090–11098.
10. Gonzalez-Anton R., Osipova M.M., Garcia-Hernandez C., Dubinina T.V., Tomilova L.G., Garcia-Cabezon C., Rodriguez-Mendez M.L. *Electrochim. Acta* **2017**, *255*, 239–247.
11. Skvortsov I.A., Kovkova U.P., Zhabanov Y.A., Khodov I.A., Somov N.V., Pakhomov G.L., Stuzhin P.A. *Dyes Pigm.* **2021**, *185*, 108944.
12. Dubinina T.V., Osipova M.M., Zasedatelev A.V., Krasovskii V.I., Borisova N.E., Trashin S.A., Tomilova L.G., Zefirov N.S. *Dyes Pigm.* **2016**, *128*, 141–148.
13. Chen Z., Xia C., Wu Y., Zuo X., Song Y. *Inorg. Chem. Commun.* **2006**, *9*, 187–191.
14. van de Winckel E., Mascaraque M., Zamarrón A., Juarranz de la Fuente Á., Torres T., de la Escosura A. *Adv. Funct. Mater.* **2018**, *28*, 1705938.
15. Tanrıverdi Eçik E., Özcan E., Kazan H.H., Erol I., Şenkuytu E., Çoşut B. *New J. Chem.* **2021**, *45*, 9984–9994.
16. Demuth J., Gallego L., Kozlikova M., Machacek M., Kucera R., Torres T., Martinez-Diaz M.V., Novakova V. *J. Med. Chem.* **2021**, *64*, 17436–17447.
17. Bernhard Y., Winckler P., Chassagnon R., Richard P., Gigot É., Perrier-Cornet J.-M., Decréau R.A. *Chem. Commun.* **2014**, *50*, 13975–13978.
18. Dowds M., Nielsen M.B. *Mol. Syst. Des. Eng.* **2021**, *6*, 6–24.
19. Morse G. E., Bender T.P. *Inorg. Chem.* **2012**, *51*, 6460–6467.
20. Winterfeld K.A., Lavarda G., Guilleme J., Guldi D.M., Torres T., Bottari G. *Chem. Sci.* **2019**, 10, 10997–11005.
21. Guilleme J., González-Rodríguez D., Torres T. *Angew. Chem. Int. Ed.* **2011**, *50*, 3506–3509.
22. Solntsev P.V., Spurgin K.L., Sabin J.R., Heikal A.A., Nemykin V.N. *Inorg. Chem.* **2012**, *51*, 6537–6547.
23. Adachi K., Watarai H. *Analyt. Chem.* **2006**, *78*, 6840–6846.
24. Khan S.U., Trashin S.A., Korostei Y.S., Dubinina T.V., Tomilova L.G., Verbruggen S.W., De Wael K. *ChemPhotoChem*, **2020**, *4*, 300–306.
25. Burtsev I.D., Dubinina T.V., Egorov A.E., Kostyukov A.A., Shibaeva A.V., Agranat A.S., Ivanova M.M., Sizov L.R., Filatova N.V., Rybkin A.Y., Varakina E.V., Bunev A.S., Antonets A.A., Milaeva E.R., Kuzmin V.A. *Dyes Pigm.* **2022**, *207*, 110690.
26. Oliveira C.P., Venturini C.G., Donida B., Poletto F.S., Guterres S.S., Pohlmann A.R. *Soft Matter* **2013**, *9*, 1141–1150.
27. Beck R.C.R., Pohlmann A.R., Guterres S.S. *J. Microencapsulation* **2004**, *21*, 499–512.
28. Radchenko A.S., Kostyukov A.A., Markova A.A., Shtil A.A., Nekipelova T.D., Borissevitch I.E., Kuzmin V.A. *Photochem. Photobiol. Sci.* **2019**, *18*, 2461–2468.
29. Oliveira A.S., Licsandru D., Boscencu R., Socoteanu R., Nacea V., Vieira Ferreira L.F. *Int. J. Photoenergy* **2009**, 2009, 413915.
30. Managa M., Mack J., Gonzalez-Lucas D., Remiro-Buenamañana S., Tshangana C., Cammidge A.N., Nyokong T. *J. Porphyrins Phthalocyanines* **2016**, *20*, 1–20.
31. Würth C., González M.G., Niessner R., Panne U., Haisch C., Genger U.R. *Talanta* **2012**, *90*, 30–37.
32. Brouwer A.M. *Pure Appl. Chem.* **2011**, *83*, 2213–2228.

Received 10.11.2022
Accepted 29.11.2022